

Polymer Physics by Quantum Computing

Cristian Micheletti^{1,*}, Philipp Hauke², and Pietro Faccioli^{3,†}

¹*Scuola Internazionale Superiore di Studi Avanzati (SISSA), Via Bonomea 265, I-34136 Trieste, Italy*

²*Physics Department of Trento University and INO-CNR BEC Center, Via Sommarive 14, I-38123 Povo (Trento), Italy*

³*Physics Department of Trento University and INFN-TIFPA, Via Sommarive 14, I-38123 Povo (Trento), Italy*

 (Received 20 April 2021; revised 21 June 2021; accepted 6 July 2021; published 19 August 2021)

Sampling equilibrium ensembles of dense polymer mixtures is a paradigmatically hard problem in computational physics, even in lattice-based models. Here, we develop a formalism based on interacting binary tensors that allows for tackling this problem using quantum annealing machines. Our approach is general in that properties such as self-avoidance, branching, and looping can all be specified in terms of quadratic interactions of the tensors. Microstates' realizations of different lattice polymer ensembles are then seamlessly generated by solving suitable discrete energy-minimization problems. This approach enables us to capitalize on the strengths of quantum annealing machines, as we demonstrate by sampling polymer mixtures from low to high densities, using the D-Wave quantum annealer. Our systematic approach offers a promising avenue to harness the rapid development of quantum machines for sampling discrete models of filamentous soft-matter systems.

DOI: [10.1103/PhysRevLett.127.080501](https://doi.org/10.1103/PhysRevLett.127.080501)

Introduction.—Despite exciting recent progress [1,2], present-day quantum computers cannot yet outperform classical ones in solving challenging physics problems of general interest. However, the current growth rate of their performance has triggered a strong effort to design new algorithmic paradigms for tackling problems that have proved hard for classical computing, and thus understand the implied advantages and disadvantages. With its wealth of problems that are inherently hard computationally, classical statistical mechanics offers an ideal avenue for such endeavors. Yet, while the potential of quantum machines has been extensively explored for quantum many-body systems [3–13], thus far there have been very few classical statistical-mechanics applications, mostly in biophysics contexts [14–18]. On the other hand, it has been shown that Monte Carlo sampling can in principle enjoy a quadratic speedup in quantum computers [19]. It is thus timely to search for high-performance implementations of sampling problems in present day quantum devices.

In this work, we discuss the use of quantum annealing machines [20–23] to tackle a paradigmatic statistical mechanics problem, namely, sampling the equilibrium ensemble of self-avoiding walks and rings, from dilute to concentrated solutions.

Generating configurations of self-avoiding polymers is an algorithmic challenge that has accompanied computational physics, and contributed to its growth, since its early days. The gist of the challenge is best illustrated for lattice embeddings of self-avoiding walks. As their chain length increases, such paths rapidly become a negligible fraction of all possible walks, thus making it impractical to sample them by discarding *a posteriori* self-crossing

conformations from a collection of random paths. The efforts that have been spent over decades to overcome this attrition problem have given rise to powerful general concepts and methods, from Monte Carlo (MC) with thermodynamic reweighting [24] to multiple Markov chains [25].

Elegant methods and strategies are now available to sample self-avoiding walks [26,27] even of considerable length [28] and enumerate them in bulk or in compact phases [29,30]. Nevertheless, efficient sampling of dense solutions or melts of self-avoiding polymers remains a major challenge for both MC and molecular dynamics simulations, because topological constraints create exceedingly long autocorrelation times.

In this work, we introduce a quadratic unconstrained binary optimization (QUBO) problem to tackle polymer sampling with quantum annealers. The Hamiltonian is chosen in such a way that its degenerate classical minima are in one-to-one correspondence with polymer configurations on a lattice. Independent realizations of polymer mixtures at any specified density can be obtained by repeated numerical minimization of the energy function.

In traditional polymer sampling strategies, the length and number of chains are set in the initial state and preserved during the subsequent stochastic evolution of the system. Instead, our QUBO model constrains the total number of monomers N and the number of bonds L in the system or, equivalently, the density (i.e., lattice filling fraction) and number of free chain ends in the mixture (see Fig. 1). The total number of chains and their lengths can instead fluctuate around their ensemble averages. Our approach can be seamlessly used to sample different statistical

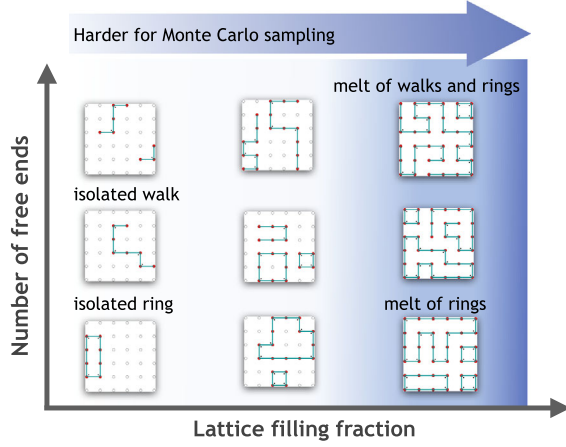


FIG. 1. The QUBO formulation of the sampling problem allows for generating mixtures of polymers with discrete degrees of freedom (here schematized for a square lattice embedding) at fixed number of monomers and free ends. The QUBO problem complexity is set by the size of the embedding space and thus is insensitive to its filling fraction.

ensembles by introducing or removing energy penalties, e.g., for branching or minimum size of admissible loops.

QUBO Hamiltonian.—Our QUBO model is defined in terms of binary tensors (BTs) of different ranks, with the tensor indices running over the sites in the embedding lattice. In a quantum annealing machine, a physical qubit is assigned to each entry of the BTs. In the logical problem, the element Γ_i of the rank-1 BT is associated to the i th site [Fig. 2(a)]. The elements Γ_{ij} of the rank-2 BT correspond to nonoriented bonds between neighboring sites i and j [Fig. 2(b)]. Analogously, the entries of the rank-3 BT, Γ_{ijk} , and the higher order ones are defined in terms of triplets or multiplets of distinct sites that yield connected paths when neighboring sites are bridged, see, e.g., Figs. 2(c) and 2(d). Each tensor entry is a binary variable that assumes the

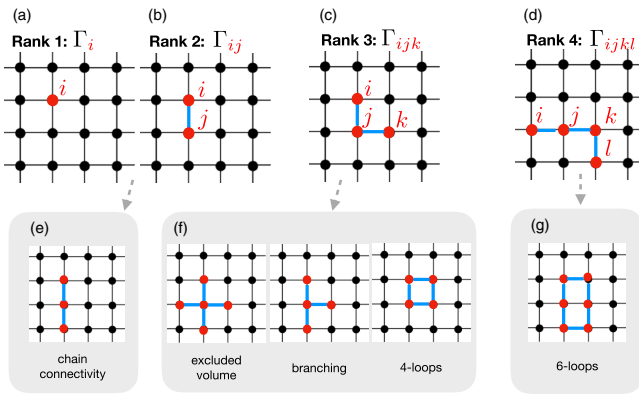


FIG. 2. Top row, (a)–(d): representation of the binary tensors, exemplified for a square lattice. Bottom row, (e)–(g): specific features or properties of the polymer chains can be specified via quadratic interactions involving tensors of appropriate rank.

values 1 or 0 if the corresponding site, bond, or n -plet is active (occupied) or inactive (empty), respectively.

We show below that by systematically adding suitable interactions between the tensors it is possible to enforce the desired physical constraints in the corresponding polymer ensemble, from the total chain lengths and chain connectivity, to self-avoidance and no branching. The Hamiltonian formulation provided hereafter is entirely general, though for simplicity we shall discuss it for square lattice embeddings. Importantly, it is formulated to involve at most quadratic functions of the BTs, as required by current quantum annealing machines [23].

The simplest polymer ensemble in this framework is generated by enforcing only the constraints of the total number of monomers and bonds, and chain connectivity. This requires only a quadratic Hamiltonian of rank-1 and rank-2 tensors, $H_0 = V_{\text{mon}} + V_{\text{bond}} + V_2$, where

$$V_{\text{mon}} = A_{\text{mon}} \left(\sum_i \Gamma_i - N \right)^2, \quad (1)$$

$$V_{\text{bond}} = A_{\text{bond}} \left(\frac{1}{2} \sum'_{i,j} \Gamma_{ij} - L \right)^2, \quad (2)$$

$$V_2 = \frac{A_2}{2} \sum'_{i,j} \Gamma_{ij} (1 - \Gamma_i). \quad (3)$$

Here and below, all coupling constants are assumed to be positive. The prime in \sum' denotes summation over distinct running indices. Upon energy minimization, interaction Eqs. (1) and (2) select polymer mixtures covering L bonds and N monomers (sites) in total. Term Eq. (3) instead enforces consistency of the chain connectivity, penalizing cases where an active bond is flanked by at least one inactive site [see Fig. 2(e)]. A sample calculation of H_0 is illustrated in the Supplemental Material [31] (SM).

As shown in Fig. 3(a), minimizing H_0 yields mixtures of lattice animals, a key class of polymers [32–34] relevant in percolation theory, too.

The degenerate ground-state manifold of H_0 thus includes configurations that are not self-avoiding and have branches. Self-intersections and branching are ruled out by complementing H_0 with two interaction terms involving the rank-3 tensor. The first term is

$$V_{\text{SA}} = \frac{A_{\text{SA}}}{5!} \sum'_{i,j,k,l,m} \Gamma_{ijk} \Gamma_{ljm}, \quad (4)$$

with the proviso that the middle index, j , refers to the interior site of the corresponding lattice trimer, see Fig. 2(c). The term in Eq. (4) penalizes cases where two active trimers share the middle site, a condition realized at crossing and branching points, see, e.g., Fig. 2(f). In addition, in analogy with Eq. (3), the consistency of active elements of the rank-3 tensor with those of lower rank, must be enforced via the following term:

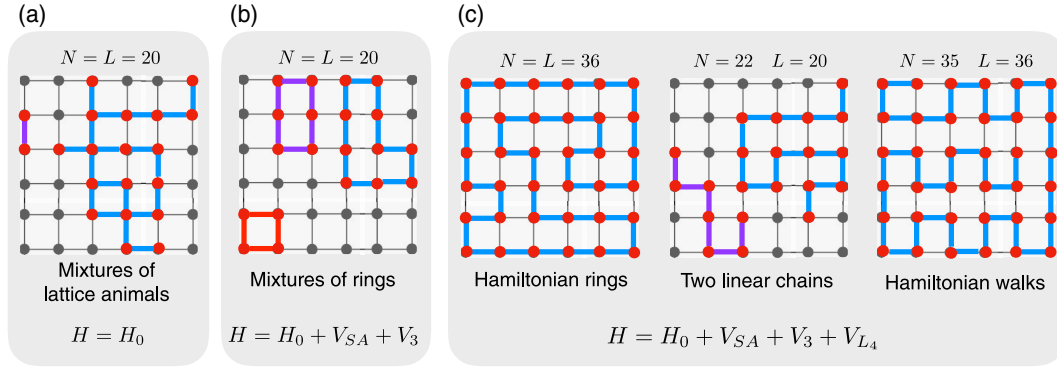


FIG. 3. Examples of the different types of polymer mixtures obtained by minimizing a suitable QUBO Hamiltonian, \mathcal{H} at different values of N and L . Panel (a): minimization of the Hamiltonian $\mathcal{H} = \mathcal{H}_0$ yields mixtures of so-called lattice animals. Panel (b): including V_{SA} and V_3 into the Hamiltonian and setting $N = L$ yields mixtures of rings. Panel (c): Further inclusion of V_{L_4} into the Hamiltonian removes loops of order 4 from sampling. Setting $N > L$ yields mixtures of rings and $N - L$ linear chains. The shown examples are for a 6×6 lattice; active sites and bonds are highlighted in color. Here, and for the results of subsequent figures, we set $A_{\text{site}} = A_{\text{bond}} = 1$, $A_2 = 2$, $A_{SA} = 5!$, $A_3 = 3!$, $A_{L_4} = 4!$.

$$V_3 = \frac{A_3}{3!} \sum_{i,j,k} [3\Gamma_{ijk} + \Gamma_{ij}\Gamma_{jk} - 2\Gamma_{ijk}(\Gamma_{ij} + \Gamma_{jk})]. \quad (5)$$

Minimizing the Hamiltonian $H = H_0 + V_{SA} + V_3$ yields the desired mixtures of self-avoiding chains with no branching. Mixtures exclusively involving ring polymers are obtained by setting $N = L$. Typical configurations at different filling fractions of a 6×6 square lattice are shown in Figs. 3(b) and 3(c), see SM for larger lattices.

Our QUBO Hamiltonian is particularly suitable for being minimized by quantum annealers, as we discuss below with a direct application on the D-Wave quantum annealing machine. We further note that the resource requirements of the QUBO model are set solely by the number of tensor elements, and not by the number of active bonds or sites, and thus dilute and dense mixtures and melts are dealt with on equal footing. In particular, in straightforward implementations of the Hamiltonian $H_0 + V_{SA} + V_3$ for a square lattice with n sites per side, the number of required qubits is $7n^2 - 10n + 4$ (see SM). Such implementation takes advantage of the fact that, for better resource efficiency, only noncollinear trimers (i.e., two bonds meeting at an angle) need to be included in interactions involving the rank-3 BT.

Mixtures of rings.—An application of our QUBO method to sample ring mixtures on a 10×10 lattice is given in Fig. 4. As the fraction of occupied lattice sites grows, the average number of rings in the mixtures and their lengths increases too, following the balance of two entropic terms. The first regards the number of distinct ring shapes, which grows approximately exponentially with the ring length, while the second is the rototranslational entropy. As density increases, it becomes advantageous to have more rings in the mixture. Indeed, the gain in rototranslational entropy of many but small rings dominates

over the loss in conformational entropy as compared to larger but fewer rings.

The sampled mixtures include instances where one or more rings are fully contained inside larger ones. Figure 4(b) shows that the probability for any ring to be involved in such nestings increases steadily with density, even at filling fractions larger than 0.6, where we find the variation of average ring length to be limited. This result could be relevant in more realistic contexts, such as adsorbates of circular DNA rings [35] or solutions of uncatenated rings [36–38], for which systematic studies for the incidence of nestings and threadings (their off-plane generalization) at varying density are not yet available.

Mixtures with linear chains.—Ring mixtures that include linear chains can be generated, too. The number of linear

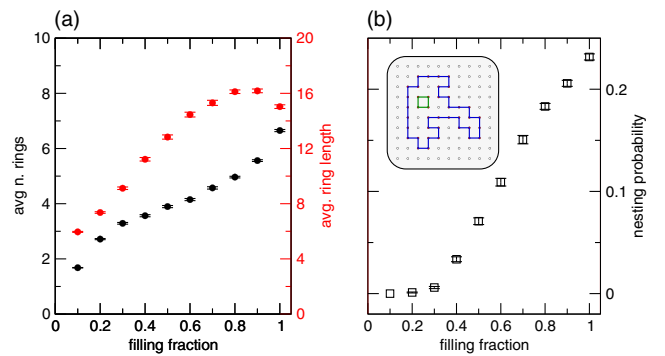


FIG. 4. (a) Average number of rings and their length in ring mixtures at varying filling fraction of a 10×10 lattice. (b) Probability that any given ring is involved in one or more nestings. At each filling density, from 1500 to 3500 samples were obtained by using a classical simulated annealer to minimize $H = H_0 + V_{SA} + V_3$ using the same interaction coefficients given in Fig. 3 and with $L = N$. The inset shows a nesting involving two rings at 0.4 filling fraction.

chains, n_l , can be specified by assigning $N = L + n_l$. The number of rings in such mixtures, as well as the contour lengths of the linear and circular chains are, again, controlled by same entropic effects discussed earlier. Low filling fractions will yield configurations that mostly consist of n_l linear chains only, see Fig. 1. Thus, at low density, setting $N = L + 1$ will mostly return individual linear chains of length L . Likewise, with $N = L$ one will mostly obtain individual rings.

We stress that our QUBO Hamiltonian is naturally formulated for sampling polydispersed ensembles of rings, with or without linear chains. However, in principle, it can be extended to generate mostly or exclusively single rings and walks even in nondilute conditions. This task can be accomplished by systematically introducing energy penalties for rings with up to $L - 1$ bonds, at the cost of increasing the number of necessary qubits.

As an illustration, we consider the suppression of the shortest possible rings consisting of four bonds, four loops in brief. In our approach, this is done by introducing the following interaction that involves the rank-3 BT:

$$V_{L_4} = \frac{A_{L_4}}{4!} \sum_{i,j,k,l} \Gamma_{ijk} \Gamma_{kli}. \quad (6)$$

This term penalizes instances where two noncollinear active trimers share the two endpoints [see last case of Fig. 2(f)]. Suppressing such loops boosts the occurrence of single-component configurations, even in the worst case scenario of Hamiltonian walks, as shown in the SM.

The elimination procedure can *in principle* be generalized to loops of any size by systematically introducing interactions with higher-rank BTs, e.g., rank-4 tensors for six loops as in Fig. 2(g), by using the recursive scheme reported in the SM. The number of higher-rank BT elements per lattice site needed to cancel loops of size $2M$ is expected to grow at most as the number of rooted self-avoiding walks of length M , which scales as $\mu^M M^{\gamma-1}$, where μ is the lattice connective constant and γ is the entropic exponent (for a square lattice $\mu \simeq 2.6$ and $\gamma \simeq 1.3$ [39,40]) see SM. For large systems, implementing such loop cancellation may require a large number of qubits. Hence, our approach based on quantum annealing and the Monte Carlo schemes based on classical computing may be regarded as complementary methods, since they are best suited and efficient for different ensembles.

Computational performance of quantum annealing.—To solve our QUBO problem using a quantum annealing machine, each entry of the BTs is assigned to a qubit. In the standard setting [20–23], the qubits are initialized in the ground state of an easily solvable Hamiltonian H_{in} that does not commute with H . Then, the system’s Hamiltonian is gradually changed with time, t , according to a given schedule $H(t) = a(t)H_{\text{in}} + b(t)H$. The functions $a(t)$ and $b(t)$ are chosen so that $a(0) = 1$ and $b(0) = 0$, while at the

end of the protocol, $t = t_{\text{sweep}}$, one has $a(t_{\text{sweep}}) = 0$ and $b(t_{\text{sweep}}) = 1$. The adiabatic theorem ensures that if the sweep $H_{\text{in}} \rightarrow H$ is sufficiently slow, the final state is the classical ground state of H , i.e., the solution of our QUBO problem. In a classical approach to our QUBO problem (based on standard simulated annealing) changes in the binary variables are accepted with the Metropolis criterion and the system’s nominal temperature is gradually lowered.

By construction, the ground state energy of our QUBO Hamiltonian is known *a priori* to be equal to 0. We used this property to compare the efficiency at minimizing H_0 of present-day hybrid quantum annealers and fully-classical simulated annealing approaches. For an equal footing comparison, we used the fully classical QUBO solver (based on classical simulated annealing) and the hybrid solver (combining quantum and classical annealing) that are available on the D-Wave machines to minimize the Hamiltonian $H_0 + V_{\text{SA}} + V_3$ at maximum filling for lattices of different size. We used default settings for the annealers and at each system size, computed the runtime $\tau_{1/2}$ required to achieve a 50% minimization success rate. The dependence of $\tau_{1/2}$ on system size for the two annealers is reported in Fig. 5.

For the addressed lattice sizes, the observed effective scaling of the hybrid annealer run-time versus system size (i.e., number of monomers) is $N^{4.2}$, which brings a significant speed up compared to scaling of the classical annealer available from D-Wave, which is $N^{5.2}$.

While the polymer mixture ensembles have no strict analog with those addressed in conventional stochastic sampling, we note that for general purpose simulation

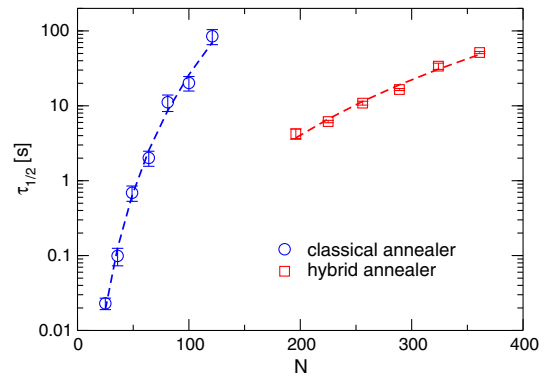


FIG. 5. Performance of the D-Wave hybrid combination of classical and quantum simulated annealers and the fully classical one at minimizing the QUBO Hamiltonian $H = H_0 + V_{\text{SA}} + V_3$ at maximum filling of square lattices with total of N sites. For each value of N , we report $\tau_{1/2}$, the run time providing a 50% success rate of reaching the ground state. See Supplemental Material and Fig. S4 for the determination of $\tau_{1/2}$ and the heuristic estimate of its confidence interval. The interpolating curves are power-law best fits to the data, and the exponents are 4.2 ± 0.2 and 5.2 ± 0.2 for the hybrid and classical cases, respectively.

strategies the autocorrelation time of dense polymeric systems is expected to scale as N^5 (from the combination of the cubic growth of the reptation time chains length, N , and the quadratic cost of computing steric interactions). The observed scaling of the quantum annealers compares well with such term of reference, even though no attempt was made to optimize the number of variables and their interactions, nor the energy gap between ground and excited states. In addition, the sizes of the systems currently addressable with hybrid annealers ($N \sim 350$), see Fig. 5, are not far from those used in conventional sampling of densely packed lattice polymers ($N \sim 2000$ [41]).

Finally, we compared the sampling of hybrid and fully classical annealers on 10×10 lattices at full filling, without observing significant differences, see Fig. S5.

Conclusions and outlook.—Applications of quantum computing to polymer physics have been few and, to our knowledge, mostly directed at lattice models of proteins for identifying the lowest-energy state of a given sequence [15–18]. In these elegant studies, however, the conformational space was not sampled, but exhaustively enumerated in advance, a feat that becomes formidable as chain length increases. In contrast, in this work, we presented a systematic theoretical framework to sample equilibrium ensembles of lattice polymer mixtures at any density.

Different physical properties, such as self-avoidance or branching, can be selected for by simply switching on or off suitable sets of interactions in a QUBO Hamiltonian. In specific applications, our general approach may be refined in order to reduce the number of required qubits, as illustrated in the SM, which also includes Refs. [42,43]. Our QUBO formulation is particularly suitable for sampling polydispersed ring melts. Our first benchmark computations on a D-Wave quantum annealer indicate a benign polynomial scaling with system size that compares well with the performance of conventional algorithms in comparable scenarios. We thus expect that the accelerating pace of quantum computing innovation will make it possible to extend our approach to more refined and larger scale models, and thus tackle challenging several systems that are of current interest. These include polymer melts where topological constraints and threadings, which generalize the nestings of Fig. 4, can hinder the system evolution and hence sampling within traditional simulation schemes.

In addition, while in this first study we focused on fully flexible homopolymers, an interesting development would be to extend our approach to semiflexible chains, and to heteropolymers. We envisage that these extensions might profit by combining quantum QUBO solvers with thermodynamic reweighting strategies performed on classical computers.

Finally, we note that sampling applications with quantum annealers have been discussed before in machine learning and other contexts [44–51]. Thus, we hope that our work can also inspire follow-up investigations

connecting the present scheme and such studies, as well as implementations on different quantum computing paradigms [52] such as Grover’s search algorithm [53], quantum Metropolis sampling [54], or quantum approximate optimization algorithms (QAOA) [55].

We thank D-Wave for granting free access to their quantum annealing machine and A. Rosa, G. Mazzola, and G. Mattiotti for useful discussions. P. H. acknowledges support by Provincia Autonoma di Trento, the Bundesministerium für Wirtschaft und Energie through the project “EnerQuant” (ProjectID 03EI1025C), and the ERC Starting Grant StrEnQTh (Project-ID 804305). P.H. and P.F. participate in the Q@TN|Quantum Science and Technology initiative in Trento.

*cristian.micheletti@sissa.it

†pietro.faccioli@unitn.it

- [1] F. Arute *et al.*, Quantum supremacy using a programmable superconducting processor, *Nature (London)* **574**, 505 (2019).
- [2] H.-S. Zhong *et al.*, Quantum computational advantage using photons, *Science* **370**, 1460 (2020).
- [3] C. Hempel, C. Maier, J. Romero, J. McClean, T. Monz, H. Shen, P. Jurcevic, B. P. Lanyon, P. Love, R. Babbush, A. Aspuru-Guzik, R. Blatt, and C. F. Roos, Quantum Chemistry Calculations on a Trapped-Ion Quantum Simulator, *Phys. Rev. X* **8**, 031022 (2018).
- [4] Y. Cao *et al.*, Quantum chemistry in the age of quantum computing, *Chem. Rev.* **119**, 10856 (2019).
- [5] A. F. Izmaylov, S. N. Genin, and I. G. Ryabinkin, Quantum chemistry quantum annealers, [arXiv:1901.04715](https://arxiv.org/abs/1901.04715).
- [6] C. Outeiral, M. Strahm, J. Shi, G. M. Morris, S. C. Benjamin, and C. M. Deane, The prospects of quantum computing in computational molecular biology, *Comput. Mol. Sci.* **11**, e1481 (2021).
- [7] S. McArdle, S. Endo, A. Aspuru-Guzik, S. C. Benjamin, and X. Yuan, Quantum computational chemistry, *Rev. Mod. Phys.* **92**, 015003 (2020).
- [8] E. F. Dumitrescu, A. J. McCaskey, G. Hagen, G. R. Jansen, T. D. Morris, T. Papenbrock, R. C. Pooser, D. J. Dean, and P. Lougovski, Cloud Quantum Computing of an Atomic Nucleus, *Phys. Rev. Lett.* **120**, 210501 (2018).
- [9] E. Zohar, J. I. Cirac, and B. Reznik, Quantum simulations of lattice gauge theories using ultracold atoms in optical lattices, *Rep. Prog. Phys.* **79**, 014401 (2016).
- [10] M. Dalmonte and S. Montangero, Lattice gauge theory simulations in the quantum information era, *Contemp. Phys.* **57**, 388 (2016).
- [11] M. C. Bañuls, R. Blatt, J. Catani *et al.*, Simulating lattice gauge theories within quantum technologies, *Eur. Phys. J. D* **74**, 165 (2020).
- [12] P. Hauke, F. M. Cucchietti, L. Tagliacozzo, I. Deutsch, and M. Lewenstein, Can one trust quantum simulators? *Rep. Prog. Phys.* **75**, 082401 (2012).
- [13] J. I. Cirac and P. Zoller, Goals and opportunities in quantum simulation, *Nat. Phys.* **8**, 264 (2012).

- [14] P. Hauke, G. Mattiotti, and P. Faccioli, Dominant Reaction Pathways by Quantum Computing, *Phys. Rev. Lett.* **126**, 028104 (2021).
- [15] A. Perdomo-Ortiz, N. Dickson, M. Drew-Brook, G. Rose, and A. Aspuru-Guzik, Finding low-energy conformations of lattice protein models by quantum annealing, *Sci. Rep.* **2**, 571 (2012).
- [16] R. Babbush, A. Perdomo-Ortiz, B. O’Gorman, W. Mcready, and A. Aspuru-Guzik, Construction of energy functions for lattice heteropolymer models: A case study in constraint satisfaction programming and adiabatic quantum optimization, *Adv. Chem. Phys.* **155**, 201 (2014).
- [17] L. H. Lu and Y. Q. Li, Quantum approach to fast protein-folding time, *Chin. Chem. Lett.* **36**, 080305 (2019).
- [18] A. Robert, P. K. Barkoutsos, S. Woerner, and I. Tavernelli, Resource-efficient quantum algorithm for protein folding, *npj Quantum Inf.* **7** (2021).
- [19] A. Montanaro, Quantum speedup of Monte Carlo methods, *Proc. R. Soc. A* **471**, 20150301 (2015).
- [20] A. Das and B. K. Chakrabarti, Colloquium: Quantum annealing and analog quantum computation, *Rev. Mod. Phys.* **80**, 1061 (2008).
- [21] T. Albash and D. A. Lidar, Adiabatic quantum computation, *Rev. Mod. Phys.* **90**, 015002 (2018).
- [22] S. E. Venegas-Andraca, W. Cruz-Santos, C. McGeoch, and M. Lanzagorta, A cross-disciplinary introduction to quantum annealing-based algorithms, *Contemp. Phys.* **59**, 174 (2018).
- [23] P. Hauke, H. G. Katzgraber, W. Lechner, H. Nishimori, and W. D. Oliver, Perspectives of quantum annealing: Methods and implementations, *Rep. Prog. Phys.* **83**, 054401 (2020).
- [24] M. N. Rosenbluth and A. W. Rosenbluth, Monte Carlo calculation of the average extension of molecular chains, *J. Chem. Phys.* **23**, 356 (1955).
- [25] M. C. Tesi, E. J. J. V. Rensburg, E. Orlandini, and S. G. Whittington, Monte Carlo study of the interacting self-avoiding walk model in three dimensions, *J. Stat. Phys.* **82**, 155 (1996).
- [26] N. Madras and A. D. Sokal, The pivot algorithm: A highly efficient monte carlo method for the self-avoiding walk, *J. Stat. Phys.* **50**, 109 (1988).
- [27] N. Clisby, Accurate Estimate of the Critical Exponent ν for Self-Avoiding Walks via a Fast Implementation of the Pivot Algorithm, *Phys. Rev. Lett.* **104**, 055702 (2010).
- [28] P. Grassberger, Pruned-enriched rosenbluth method: Simulations of θ polymers of chain length up to 1 000 000, *Phys. Rev. E* **56**, 3682 (1997).
- [29] A. R. Conway and A. J. Guttmann, Square Lattice Self-Avoiding Walks and Corrections to Scaling, *Phys. Rev. Lett.* **77**, 5284 (1996).
- [30] J. L. Jacobsen, Unbiased Sampling of Globular Lattice Proteins in Three Dimensions, *Phys. Rev. Lett.* **100**, 118102 (2008).
- [31] See Supplemental Material at <http://link.aps.org/supplemental/10.1103/PhysRevLett.127.080501> for additional information about numerical and analytic calculations and further numerical results comparing sampling by classical and quantum annealing.
- [32] G. Parisi and N. Sourlas, Critical Behavior of Branched Polymers and the Lee-Yang Edge Singularity, *Phys. Rev. Lett.* **46**, 871 (1981).
- [33] A. Rosa and R. Everaers, Ring Polymers in the Melt State: The Physics of Crumpling, *Phys. Rev. Lett.* **112**, 118302 (2014).
- [34] R. Everaers, A. Y. Grosberg, M. Rubinstein, and A. Rosa, Flory theory of randomly branched polymers, *Soft Matter* **13**, 1223 (2017).
- [35] G. Witz, K. Rechendorff, J. Adamcik, and G. Dietler, Conformation of Ring Polymers in 2D Constrained Environments, *Phys. Rev. Lett.* **106**, 248301 (2011).
- [36] D. Michieletto, D. Marenduzzo, E. Orlandini, G. P. Alexander, and M. S. Turner, Threading dynamics of ring polymers in a gel, *ACS Macro Lett.* **3**, 255 (2014).
- [37] J. Smrek and A. Y. Grosberg, Minimal surfaces on unconcatenated polymer rings in melt, *ACS Macro Lett.* **5**, 750 (2016).
- [38] J. Smrek, K. Kremer, and A. Rosa, Threading of unconcatenated ring polymers at high concentrations: Double-folded vs time-equilibrated structures, *ACS Macro Lett.* **8**, 155 (2019).
- [39] A. J. Guttmann and A. R. Conway, Square lattice self-avoiding walks and polygons, *Ann. Comb.* **5**, 319 (2001).
- [40] I. Jensen, Enumeration of self-avoiding walks on the square lattice, *J. Phys. A* **37**, 5503 (2004).
- [41] N. Kinney, M. Hickman, R. Anandakrishnan, and H. R. Garner, Crossing complexity of space-filling curves reveals entanglement of s-phase dna, *PLoS One* **15**, e0238322 (2020).
- [42] M. Leib, P. Zoller, and W. Lechner, A transmon quantum annealer: Decomposing many-body ising constraints into pair interactions, *Quantum Sci. Technol.* **1**, 015008 (2016).
- [43] R. Babbush, B. O’Gorman, and A. Aspuru-Guzik, Resource efficient gadgets for compiling adiabatic quantum optimization problems, *Ann. Phys. (Amsterdam)* **525**, 877 (2013).
- [44] S. H. Adachi and M. P. Henderson, Application of quantum annealing to training of deep neural networks, *arXiv*: 1510.06356.
- [45] S. Szoke, W. Vinci, G. Aeppli, and P. A. Warburton, Maximum-entropy inference with a programmable annealer, *Sci. Rep.* **6**, 22318 (2016).
- [46] M. Benedetti, J. Realpe-Gómez, R. Biswas, and A. Perdomo-Ortiz, Quantum-Assisted Learning of Hardware-Embedded Probabilistic Graphical Models, *Phys. Rev. X* **7**, 041052 (2017).
- [47] L. M. Sieberer and W. Lechner, Programmable superpositions of ising configurations, *Phys. Rev. A* **97**, 052329 (2018).
- [48] W. Vinci, L. Buffoni, H. Sadeghi, A. Khoshaman, E. Andriyash, and M. H. Amin, A path towards quantum advantage in training deep generative models with quantum annealers, *arXiv*:1912.02119.
- [49] M. S. Könz, G. Mazzola, A. J. Ochoa, H. G. Katzgraber, and M. Troyer, Uncertain fate of fair sampling in quantum annealing, *Phys. Rev. A* **100**, 030303(R) (2019).

- [50] M. Yamamoto, M. Ohzeki, and K. Tanaka, Fair sampling by simulated annealing on quantum annealer, *J. Phys. Soc. Jpn.* **89**, 025002 (2020).
- [51] V. Kumar, C. Tomlin, C. Nehrkorn, D. O'Malley, and J. Dulny III, Achieving fair sampling in quantum annealing, [arXiv:2007.08487](https://arxiv.org/abs/2007.08487).
- [52] E. Zahedinejad and A. Zaribafiyani, Combinatorial optimization on gate model quantum computers: A survey, [arXiv:1708.05294](https://arxiv.org/abs/1708.05294).
- [53] W. P. Baritempa, D. W. Bulger, and G. R. Wood, Grover's quantum algorithm applied to global optimization, *SIAM J. Optim.* **15**, 1170 (2005).
- [54] K. Temme, T. J. Osborne, K. G. Vollbrecht, D. Poulin, and F. Verstraete, Quantum metropolis sampling, *Nature (London)* **471**, 87 (2011).
- [55] E. Farhi, J. Goldstone, and S. Gutmann, A quantum approximate optimization algorithm, [arXiv:1411.4028](https://arxiv.org/abs/1411.4028).